ISSN 1070-4272, Russian Journal of Applied Chemistry, 2020, Vol. 93, No. 12, pp. 1931–1939. © Pleiades Publishing, Ltd., 2020.

COMPOSITE MATERIALS

A Novel Phosphorus/Silicon-Containing Flame Retardant—Functionalized Graphene Nanocomposite: Preparation, Characterization and Flame Retardancy

Jiangbo Wang[a],*

[a] *School of Materials and Chemical Engineering, Ningbo University of Technology, Ningbo, Zhejiang, 315211 China*
**e-mail: jiangbowang@163.com*

Received August 24, 2020; revised November 16, 2020; accepted November 18, 2020

Abstract—A novel compound (DOPO-V-PA) containing phosphorus and silicon elements was grafted onto the surface of graphene oxide (GO) to obtain a graphene-based flame retardant (GO–DOPO-V-PA). The structure of GO-DOPO-V-PA was characterized and confirmed by FTIR and XPS spectra. AFM measurements showed that the average height of GO-DOPO-V-PA was thicker than that of GO and that the surface of GO-DOPO-V-PA was not uniform, contrary to the surface of the initiator GO before modification. The thermal stability of GO-DOPO-V-PA was greatly improved by the functionalization of GO with DOPO-V-PA, and the residual char of GO-DOPO-V-PA at 600°C increased from 16.45 (GO) to 61.44 wt %. After GO-DOPO-V-PA was incorporated into epoxy resin (EP), the residual char of EP/GO-DOPO-V-PA was almost 3 wt % higher than that of pure EP and EP/GO. Furthermore, EP/GO-DOPO-V-PA exhibited excellent flame retardancy. Compared to the pure EP and EP/GO, the peak heat release rate (pHRR) and total heat release (THR) of EP/GO-DOPO-V-PA both decreased, which was probably caused by the higher residual char of EP/GO-DOPO-V-PA during combustion. Thus, the flame retardancy of the graphene-based composites was improved with the addition of 2 wt % GO-DOPO-V-PA, which was much less than the previously known flame retardant systems, and the graphene has been demonstrated its excellent performance in the fire safety of the polymer materials.

Keywords: graphene oxide, functionalization, P/Si flame retardant, epoxy resin

DOI: 10.1134/S1070427220120162

INTRODUCTION

Epoxy resin (EP) is a very important thermosetting material and has been widely used in paints, laminates, adhesives, printed circuit boards and insulating materials for electric devices due to its excellent mechanical and chemical properties [1–6]. However, the susceptibility of EP to fire is still a great concern. The use of flame retardants allows improvement inthe fire behavior of EP and fulfills the requirements in the application of electronic fields [7–11].

With ultrahigh thermal, mechanical, electrical and gas barrier properties, graphene has attracted considerable attention from industrial to academic fields [12–15]. Over the past few years, graphene oxide and its derivatives have shown great potential for fire safety applications of polymers, and a significant enhancement of flame retardancy is achieved by introducing very low amounts of graphene into the polymer matrix [16–20]. However, due to the intrinsic vander Waals forces and its high surface area, the aggregation and restacking phenomena of graphene limit its application in polymer materials [21, 22]. After oxidation, oxygen-containing groups (such as hydroxyl, epoxide, carboxyl, etc.) are present on the surface and the edges of graphene sheets. Thus, in the conventional method, organic compounds are grafted onto the surface of graphene sheets, which improves the dispersion of graphene in the polymer matrix but usually deteriorates the flame retardancy of materials [23–25]. This problem can be

solved by covalently modifyingthe flame retardants to simultaneously improve the dispersion and flame retardancy. To achieve this objective, various halogen-free flame retardants, including phosphorus, silicon, and nitrogen compounds, have been developed to modify graphene sheets in recent years [26–35].

Herein, a novel strategy based on functionalized graphene oxide is developed. A flame retardant containing phosphorus and silicon elements is synthesized and subsequently grafted onto the surface of graphene oxide. The structure and morphology of functionalized graphene oxide (GO-DOPO-V-PA) are characterized by FTIR, XPS and AFM measurements. Then, GO-DOPO-V-PA is incorporated into EP to fabricate EP nanocomposites with a low GO-DOPO-V-PA loading. The combustion and thermal properties of EP/GO-DOPO-V-PA composites are evaluated by cone calorimetry and TGA measurements.

EXPERIMENTAL

Material. Graphite powders (spectrum pure), concentrated sulfuric acid (98%), phosphoric acid (85%), potassium permanganate, hydrogen peroxide (30%), tetramethylammonium hydroxide (TMAOH), (3-aminopropyl)trimethoxysilane (APT), 2,2′-azobisisobutyronitrile (AIBN), *N,N*'-dicyclohexylcarbodiimide (DCC) and tetrahydrofuran (THF) were purchased from Alfa Aesar Chemical Reagent Co., Ltd. 9,10-Dihydro-9-oxa-10-phosphaphenanthrene-10-oxide (DOPO) was purchased from TCI Development Co., Ltd. Vinyltrimethoxysilane (VTMS) and benzene (reagent grade) werepurchased from Sigma-Aldrich Co., Ltd. Ethyl alcohol was supplied by Decon. Phenyltrimethoxysilane (PTMS) (reagent grade) was purchased from Gelest Chemical Reagent Co., Ltd. Chloroform ($CHCl_3$) and hydrochloric acid were supplied by Fisher Scientific Chemical Co. EPON 826 with an epoxy equivalent weight of 178-186 grams was supplied by Hexion and used as received. The hardener Jeffamine D230, with an amine equivalent weight of 60 grams, was supplied by Huntsman Co., Ltd., and used as received.

Synthesis of DOPO-V-PA. DOPO (21.6 g, 0.1 mol), VTMS (14.8 g, 0.1 mol), and benzene (100 mL) were added to a three-necked flask with a mechanical stirrer, flux condenser, dropping funnel, and nitrogen inlet. After the mixture was saturated with nitrogen atmosphere under vigorous mechanical stirring, the temperature was increased to 80°C. After the DOPO was dissolved completely, 0.1 g of AIBN, which was predissolved in 50 mL of benzene, was slowly added to the above reaction vessel within 2 h at 80°C, and the mixture wasmaintained at 80°C for 24 h. Afterwards, the product was purified by filtering. Then, benzene was removed by rotary evaporation, yielding a colorless liquid product named DOPO-V [36].

As shown in Fig. 1, DOPO-V-PA was synthesized by hydrolysis and condensation reactions as follows: distilled water (25 mL), EtOH (75 mL) and TMAOH (1 mL) were mixed in a 250-mL flask under stirring. A mixture of PTMS, APS and DOPO-V at a certain molar ratio (70 : 10 : 20) was added to the above solution, maintaining a 10% weight percentage. Stirring was stopped after 8 h, and the solution was aged at room temperature overnight. The precipitated condensate was collected by decantation of the clearest supernatant, washed by vacuum filtration with distilled H_2O/EtOH (1/3 by volume), and then washed again in pure EtOH. The rinsed powder (DOPO-V-PA) was dried thoroughly under vacuum for 20 h at room temperature.

Functionalization of GO. GO was prepared from graphite by a modified Hummers' method [37]. GO contains hydroxyl functional groups on its basal planes and edges, which provide active sites to react with silane. Briefly, the as-prepared GO (0.2 g) was first suspended in DMF (200 mL) in a 500-mL three-neck flask by ultrasonication for 90 min. Subsequently, DOPO-V-PA (0.8 g) and DCC (0.1 g, as cat.) were added to the flask containing the GO, followed by ultrasonication for 30 min. The mixture was heated to 70°C under stirringand refluxed for 20 h under a nitrogen atmosphere. Afterwards, the mixture was centrifuged and thoroughly washed with DMF and anhydrous THF to remove the residual DOPO-V-PA. Then, the product, DOPO-V-PA-functionalized graphene sheets (GO-DOPO-V-PA), was dried under vacuum at room temperature for 12 h to remove the solvent (Fig. 1).

Preparation of epoxy nanocomposite. Briefly, the EP/GO-DOPO-V-PA composites were prepared as follows: GO-DOPO-V-PA (2 g) was dispersed in acetone and sonicated for 60 min to form a uniform

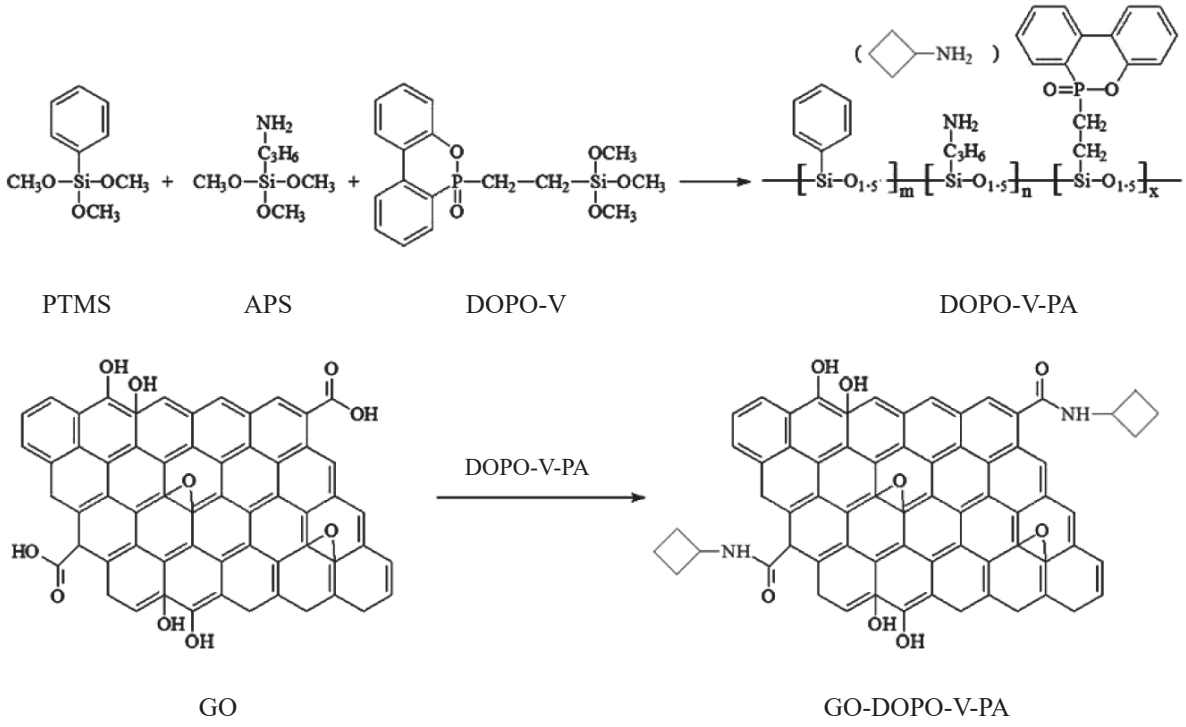

Fig. 1. Synthesis route of GO-DOPO-V-PA.

black suspension. Then, EPON 826 (73.5 g) was added to the mixture and dispersed by a mechanical stirrer for 30 min. The mixture was heated in a vacuum oven at 50°C for 10 h to remove the solvent. After that, D230 (24.5 g) was added to the mixture and stirred for 30 min. After degassing in a vacuum for 10 min to remove air, the samples were cured at 80 °C for 2 h and postcured at 135°C for 2 h. For comparison, pure epoxy (EP) and 2 wt % GO/epoxy (EP/GO) composites were also prepared under the same processing conditions.

Characterization and measurements. The Fourier transform infrared (FTIR) spectra of the dried samples were recorded using a Digilab Scimitar FTS-2000 IR spectrometer.

X-ray photoelectron spectroscopy (XPS) was carried out with a Thermo Scientific ESCALAB 250Xi X-ray photoelectron spectrometer equipped with a monochromatic AlK_{α} X-ray source (1486.6 eV).

AFM observation was performed on the Bruker Dimension Icon atomic force microscope in tappingmode. The aqueous GO suspension and the DMF suspension of GO-DOPO-V-PA were spin-coated onto freshly cleaned silica surfaces.

Thermogravimetric analysis (TGA) was carried out with a TA instrument Q500 thermogravimetric analyzer. The sample (approximately 10 mg) was heated from 50 to 600°C (or 800°C) at a 10°C/min heating ramp rate under a nitrogen atmosphere.

The cone calorimeter measurement was performed with the Govmark CC-1 cone instrument according to ASTM E 1354 using a cone-shaped heater with an incident flex set at 50 Kw/m^2. The dimensions of each specimen were 100 × 100 × 3 mm^3.

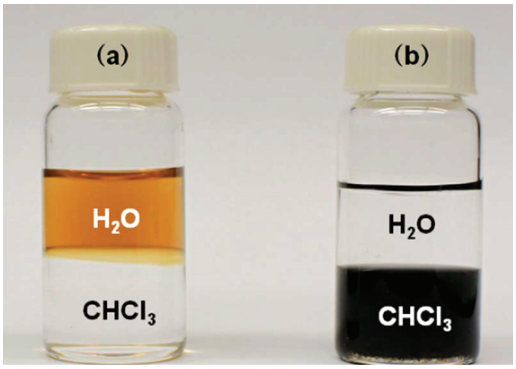

Fig. 2. Solubility of (a) GO and (b) GO-DOPO-V-PA.

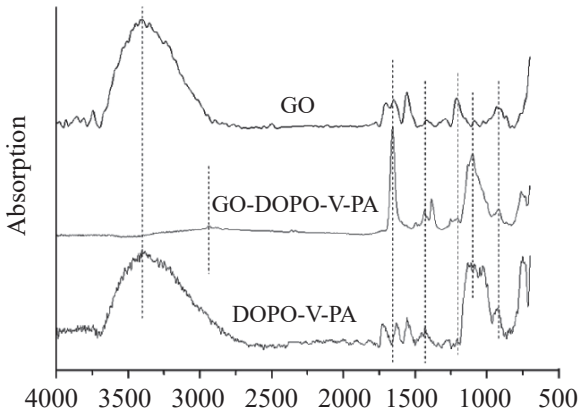

Fig. 3. FTIR spectra of GO, DOPO-V-PA, and GO-DOPO-V-PA.

RESULTS AND DISCUSSION

Structural and morphological characterization. Figure 2 shows digital photos of the solubility of GO and GO-DOPO-V-PA in an insoluble mixture of water and chloroform. GO is hydrophilic due to the presence ofcarboxylic, epoxy, carbonyl and hydroxide groups on its surface andedges and was therefore easily dispersed in water (Fig. 2a). After surface functionalization of GO with DOPO-V-PA, the strong interaction between DOPO-V-PA and chloroform caused GO-DOPO-V-PA to change from being hydrophilic to hydrophobic and to become soluble in chloroform, as shown in Fig. 2b. The phase transfer behavior of the GO starting material from water to chloroform upon the formation of the GO-DOPO-V-PA hybrid can be considered a sign of GO reduction [38].

The FTIR spectra of GO, DOPO-V-PA and GO-DOPO-V-PA are shown in Fig. 3. Most of the characteristic absorbance peaks of the oxygen-containing groups (e.g., –OH at 3408 cm^{-1}, C=O at 1705 cm^{-1}, and C–O at 1211 cm^{-1}) were detectedin the spectrum of GO. In the spectrum of GO-DOPO-V-PA, the peaks at 1099 and 916 cm^{-1} were attributed to Si–O–Si bonds and P–O–Ph bonds, respectively. Moreover, the peaks at approximately 2940 cm^{-1} and 1433 cm^{-1}

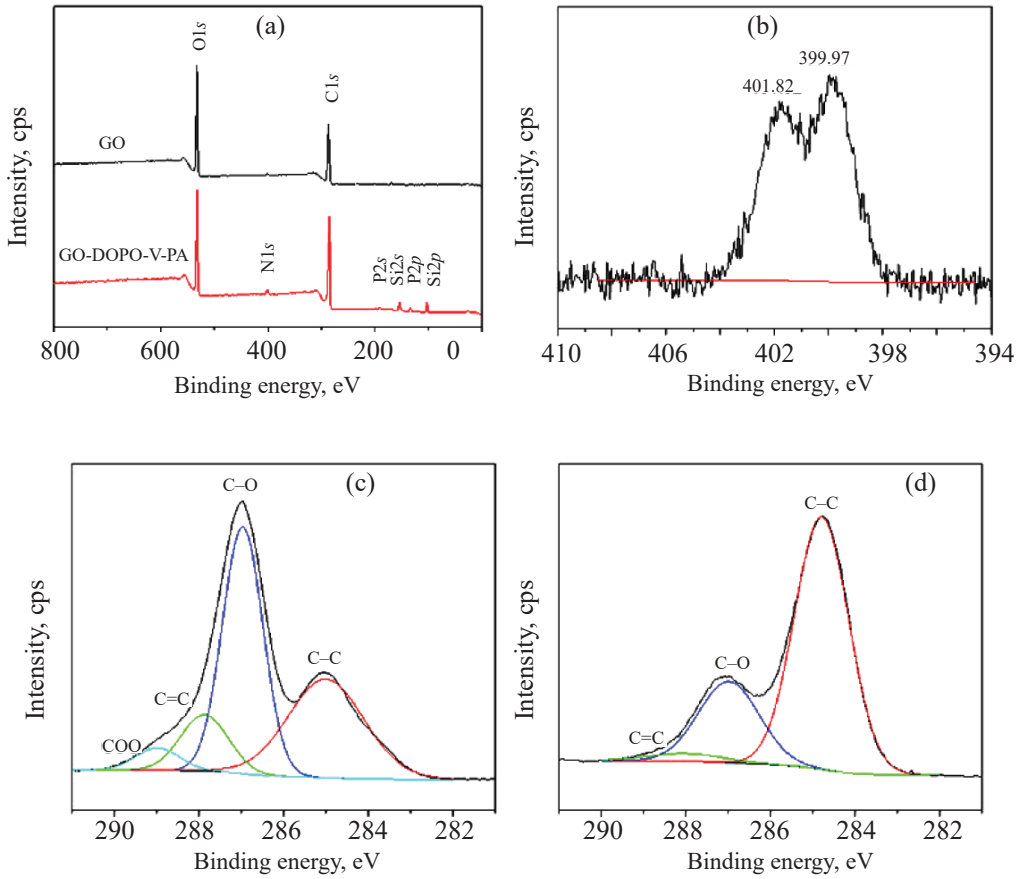

Fig. 4. (Color online) (a) XPS survey of GO and GO- DOPO-V-PA and high-resolution XPS spectra of (b) N1*s* for GO-DOPO-V-PA, (c) C1*s* for GO, and (d) C1*s* for GO-DOPO-V-PA.

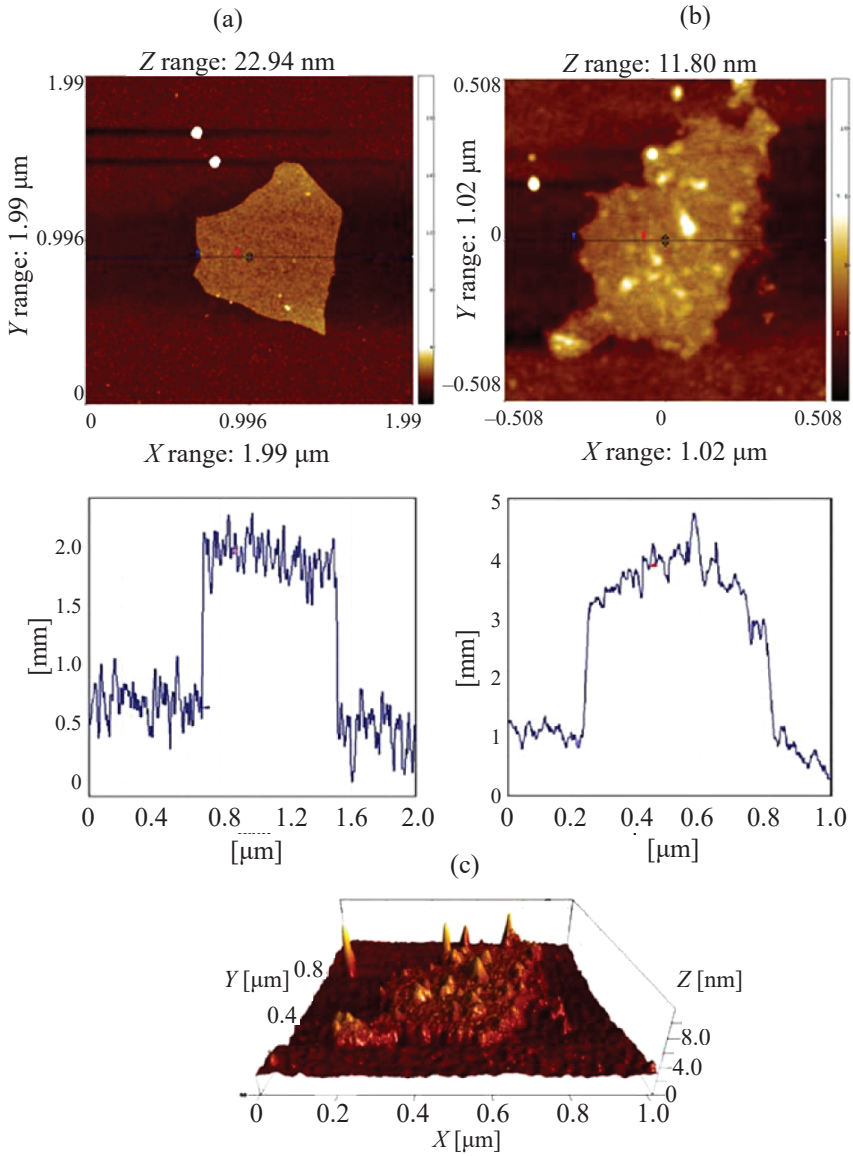

Fig. 5. (Color online) AFM images of (a) GO and (b) 2D, (c) 3D of GO- DOPO-V-PA.

represented the asymmetric and symmetric vibrations of $–CH_2–$, and the peak at 1203 cm^{-1} represented the P=O bending. These results indicate that DOPO-V-PA was successfully grafted onto GO.

Further evidence of the successful GO functionalization with DOPO-V-PA was provided by the XPS spectra, as shown in Fig. 4. Comparison of the XPS survey spectra of GO and GO-DOPO-V-PA (Fig. 4a) revealed the lack of Si, P and N signals in the GO sample, which appeared in the GO-DOPO-V-PA sample. The new peaks at binding energies of 401.4, 190.4, 154.4, 133.4, and 103.4 eV in the XPS spectra of GO-DOPO-V-PA were attributed to the N1*s*, P2*s*, Si2*s*,

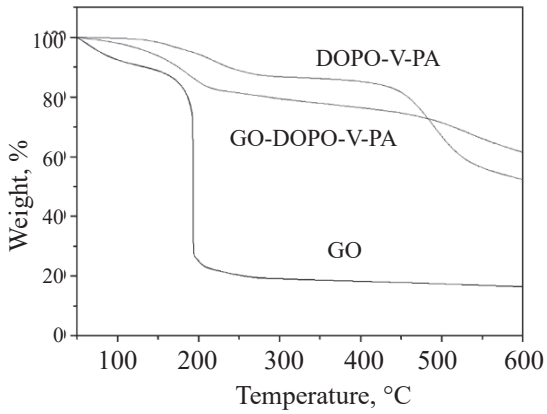

Fig. 6. TGA curves of GO, DOPO-V-PA and GO-DOPO-V-PA.

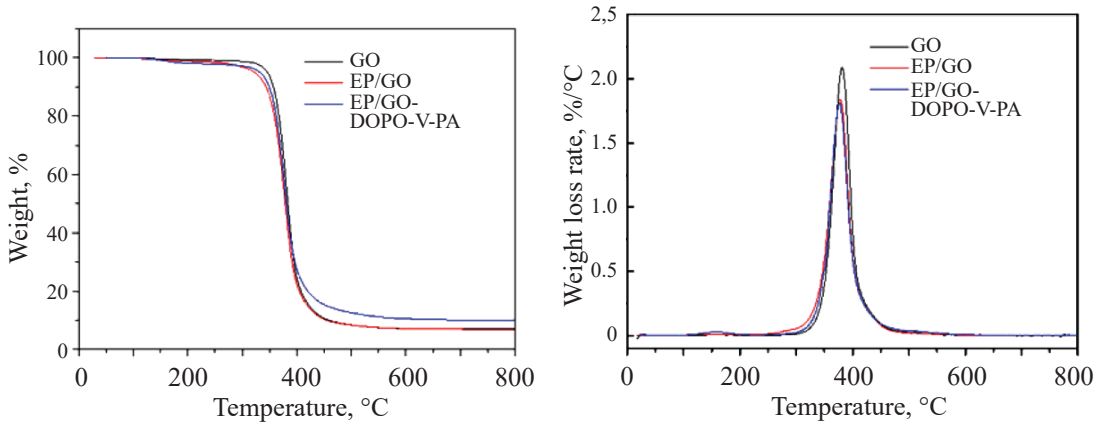

Fig. 7. (Color online) TGA and DTG curves of EP composite.

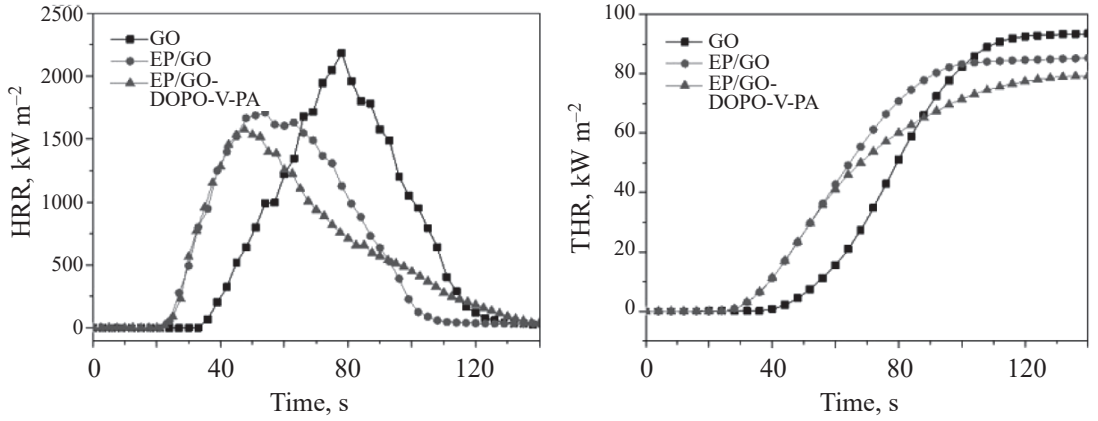

Fig. 8. HRR and THR curves of EP, EP/GO and EP/GO-DOPO-V-PA.

P2*p*, and Si2*p*, respectively. The presence of silicone, phosphorus and nitrogen elements was due to DOPO-V-PA.

The C1*s* XPS spectra for GO are shown in Fig. 4b. The peaks at 285.0, 287.0, 287.9, and 289.0 eV were assigned to the carbon atoms in C–C, C–O, C=O, and COO, respectively. After functionalization of GO, the oxygen-containing functionality of C–O decreased, and the peak of COO at 289.0 eV mostly disappeared in the GO-DOPO-V-PA spectrum in Fig. 4d, which originated from the formation of a C–O–N bond by the surface modification of GO. Notable changes in the binding energy and intensity were detected in the C1*s* XPS spectra of GO, which could be attributed to the functionalization of GO with DOPO-V-PA. Figure 4b shows the high-resolution XPS spectra of N1*s* for GO-DOPO-V-PA. The N1*s* band of GO-DOPO-V-PA was located at 400.0 eV (C–N) and 401.8 eV (CO–N), in good agreement with previous work [39, 40], which further proved that GO was modified with DOPO-V-PA through the esterification reaction.

The morphology of GO and GO-DOPO-V-PA was investigated by AFM measurements. As shown in Fig. 5a, the height of the GO sheet was approximately 1 nm, indicating that the exfoliation of graphite to individual GO nanosheets was indeed achieved. Moreover, upon grafting DOPO-V-PA onto GO, the average height of GO-DOPO-V-PA in Fig. 5b was approximately 2–4 nm, which was thicker than the height of the GO sheet. The increase in the thickness of GO-DOPO-V-PA was attributed to the presence of functionalized DOPO-V-PA chains grafted on the graphene sheets. The 3D image of GO-DOPO-V-PA revealed that the grafted DOPO-V-PA chains on the GO surface were not uniform, contrary to the uniform surface distribution of initiator GO before modification. A similar result has also been observed for the thickness of functionalized graphene sheets by AFM measurements [41].

Table 1 TGA data of EP, EP/GO and EP/GO-DOPO-V-PA

Sample	Temperature (°C)		Peak rate, wt %/°C	Residual charh, wt %
	$T_{5wt\%}$	T_{max}		
EP	346.0	381.4	2.09	7.02
EP/GO	322.5	378.2	1.84	6.95
EP/GO-DOPO-V-PA	332.5	376.9	1.81	10.00

To investigate the thermal stability of GO, DOPO-V-PA and GO-DOPO-V-PA, TGA measurementswere carried out under a nitrogen atmosphere, as shown in Fig. 6. The temperature at which the weight loss reached 5 wt % was defined as the initial decomposition temperature, which was denoted as $T_{5wt\%}$; the temperature at which the degradation rate reached a maximum was defined as T_{max}. The T_{max} of GO was approximately 200 °C, which was caused by the thermal decomposition of labile oxygen functional groups. For GO-DOPO-V-PA, the $T_{5wt\%}$ increased from 78.5 (GO) to 138.5 °C, indicating that the labile oxygen groups in GO were partly removed after grafting with DOPO-V-PA. Moreover, the residual char of GO-DOPO-V-PA at 600°C increased from 16.45 wt % (GO) to 61.44 wt %. Thus, the thermal stability of GO-DOPO-V-PA was improved significantly by the functionalization of GO with DOPO-V-PA.

Thermal stability. The TGA and DTG curves of EP composites are shown in Fig. 7, and the corresponding data are summarized in Table 1. For EP/GO, $T_{5wt\%}$ and T_{max} were both lower than those of pure EP because GO was thermally unstable and its major thermal decomposition process occurred at approximately 200°C. Moreover, the peak rates of EP/GO at T_{max} and residual char at 800°C were also lower than those of pure EP. After the addition of GO-DOPO-V-PA to EP, anoticeable change in the thermal stability was found. The residual char of EP/GO-DOPO-V-PA at 800°C was 10.00 wt %, which was almost 3 wt % higher than the residual char of pure EP and EP/GO. The DOPO-V-PA generated a stable char layer on the surface of EP in combustion, which reinforced the barrier effect of the graphene sheets. Combining these results with the TGA results, it can be concluded that the thermal stability of graphene-based EP nanocomposites was greatly improved by the chemical reduction.

Flame retardancy. Figure 8 shows the HRR and THR curves of EP, EP/GO and EP/GO-DOPO-V-PA. With a GO loading of 2 wt %, the peak heat release rate (pHRR) and total heat release (THR) of EP decreased by approximately 21.6 % (from 2180.8 to 1710.4 KW/m^2) and 8.9% (from 93.6 to 85.3 MJ/m^2), respectively. A similar trend was observed for EP/GO-DOPO-V-PA, and GO-DOPO-V-PA exhibited much better flame retardancy than GO. Comparing 2 wt% GO loading and GO-DOPO-V-PA, the values of pHRR and THR decreased by 7.9% (from 1710.4 to 1574.9 KW/m^2) and 6.9% (from 85.3 to 79.4 MJ/m^2), respectively, which was probably caused by the higher residual char during combustion.

CONCLUSIONS

In this work, a novel functionalized graphene oxide (GO-DOPO-V-PA) containing phosphorus and silicon elements was synthesized and used as a graphene-based flame retardant in EP nanocomposites. The FTIR, XPS and AFM results indicated that DOPO-V-PA was successfully grafted onto the surface of the graphene sheets. GO-DOPO-V-PA was hydrophobicand could easily be dissolved in chloroform. The TGA measurement showed that the thermal stability of the graphene sheets was notably improved by the functionalization of GO with DOPO-V-PA, and the residual char at 600°C increased from 16.45 wt % (GO) to 61.44 wt %. Furthermore, the residual char of EP/GO-DOPO-V-PA was almost 3 wt % higher than that of pure EP and EP/GO. Compared to the pure EP and EP/GO, the pHRR and THR of EP/GO-DOPO-V-PA both decreased, which was probably caused by the higher residual char of EP/GO-DOPO-V-PA during combustion. Thus, the flame retardancy of the graphene-based composites was improved with the addition of 2 wt % GO-DOPO-V-PA, which was much less than the previously known flame retardant systems, and the graphene has been demonstrated its excellent performance in the fire safety of the polymer materials.

ACKNOWLEDGMENTS

The author wishes to thank the National Natural Science Foundation of China (51703099), Natural Science Foundation

of Zhejiang Province (LQ13E030002) and Ningbo Natural Science Foundation (2019A610032) for financial support. This work was also supported by Shanghai Key Laboratory of Multiphase Materials Chemical Engineering.

CONFLICT OF INTEREST

The authors declare that they have no conflicts of interest requiring disclosure in this paper.

REFERENCES

1. Zhai, C.C., Xin, F., and Chen, Y., *Polym. Advan. Technol.*, 2019, vol. 30, no. 11, pp. 2833–2845. https://doi.org/10.1002/pat.4716
2. You, G., Cheng, Z., and Tang, Y., *Ind. Eng. Chem. Res.*, 2015, vol. 54, no. 30, pp. 7309–7319. https://doi.org/10.1021/acs.iecr.5b00315
3. Gu, H., Ma, C., and Gu, J., *J. Mater. Chem. C*, 2016, vol. 4, pp. 5890–5906. https://doi.org/10.1039/C6TC01210H
4. Huang, H., Zhang, K., and Jiang, J., *Polym. Int.*, 2017, vol. 66, pp. 85–91. https://doi.org/10.1002/pi.5244
5. Tan, Y., Shao, Z.B., and Chen, X.F., AC*S Appl. Mater. Interfaces*, 2015, vol. 7, no. 32, pp. 17919–17928. https://doi.org/10.1021/acsami.5b04570
6. Liu, S., Fang, Z.P., and Yan, H.Q., *RSC Adv.*, 2016, vol. 6, pp. 5288–5295. https://doi.org/10.1039/C5RA25988F
7. Zhao, X., Babu, H.V., and Llorca, J., *RSC Adv.*, 2016, vol. 6, pp. 59226–59236. https://doi.org/10.1039/C6RA13168A
8. Kalali, E.N., Wang, X., and Wang, D.Y., *J. Mater. Chem. A*, 2015, vol. 3, pp. 6819–6826. https://doi.org/10.1039/C5TA00010F
9. Yu, B., Xing, W.Y., and Guo, W.W., *J. Mater. Chem. A*, 2016, vol. 4, pp. 7330–7340. https://doi.org/10.1039/C6TA01565D
10. Levchik, S.V., and Weil, E.D., *Polym. Int.*, 2004, vol. 53, pp. 1901–1929. https://doi.org/10.1002/pi.1473
11. Yang, S., Wang, J., and Huo, S.Q., *Polym Degrad. Stab.*, 2016, vol. 128, pp. 89–98. https://doi.org/10.1016/j.polymdegradstab.2016.03.017
12. Hu, K., Kulkarni, D.D., and Choi, I., *Prog. Polym. Sci.*, 2014, vol. 39, no. 11, pp. 1934–1972. https://doi.org/10.1016/j.progpolymsci.2014.03.001
13. Hersam, M.C., *Acs Nano*, 2015, vol. 9, no. 5, pp. 4661–4663. https://doi.org/10.1021/acsnano.5b02806
14. Rao, C.N.R., Sood, A.K., and Subrahmanyam, K.S., *Angew. Chemie*, 2009, vol. 40, no. 52, pp. 7752–7777. https://doi.org/10.1002/anie.200901678
15. Zhu, Y.W., Murali, S., and Cai, W.W., *Adv. Mater.*, 2010, vol. 22, pp. 3906–3924. https://doi.org/10.1002/adma.201001068
16. Guo, Y., Bao, C., and Song, L., *Ind. Eng. Chem. Res.*, 2011, vol. 50, no. 13, pp. 7772–7783. https://doi.org/10.1021/ie200152x
17. Potts, J.R., Dreyer, D.R., and Bielawski, C.W., *Polymer*, 2011, vol. 52, no. 1, pp. 5–25. https://doi.org/10.1016/j.polymer.2010.11.042
18. Ming, G., Li, J.F., and Zhang, X.Q., *Combust. Sci. Technol.*, 2018, vol. 190, no. 6, pp. 1126–1140. https://doi.org/10.1080/00102202.2018.1437727
19. Sun, Y., Li, C., and Xu, Y., *Chem. Commun.*, 2010, vol. 46, no. 26, pp. 4740–4742. https://doi.org/10.1039/c001635g
20. Gui, H., Xu, P., and Hu, Y.D., *Rsc Adv.*, 2015, vol. 5, pp. 27814–27822. https://doi.org/10.1039/c4ra16393a
21. Ramanathan, T., Abdala, A.A., and Stankovich, S., *Nat. Nanotech.*, 2008, vol. 3, pp. 327–331. https://doi.org/10.1038/nnano.2008.96
22. Zhu, J., *Nat. Nanotech.*, 2008, vol. 3, pp. 528–529. https://doi.org/10.1038/nnano.2008.249
23. Wang, Y., Shi, Z., and Fang, J., *Carbon*, 2011, vol. 49, no. 4, pp. 1199–1207. https://doi.org/10.1016/j.carbon.2010.11.036
24. Hou, S., Su, S., and Kasner, M.L., *Chem. Phys. Lett.*, 2010, vol. 501, no. 1–3, pp. 68–74. https://doi.org/10.1016/j.cplett.2010.10.051
25. Wu, W.Q., Xu, Y.T., and Wu, H.Y., *J. Appl. Polym. Sci.*, 2020, vol. 137, no. 1, p. 47710. https://doi.org/10.1002/app.47710
26. Attia, N.F., Abd El-Aal, N.S., and Hassan, M.A., *Polym. Degrad. Stab.*, 2016, vol. 126, pp. 65–74. https://doi.org/10.1016/j.polymdegradstab.2016.01.017
27. Yu, B., Shi, Y.Q., and Yuan, B.H., *J. Mater. Chem. A*, 2015, vol. 3, pp. 8034–8044. https://doi.org/10.1039/c4ta06613h
28. Huang, X., Qi, X., and Boey, F., *Chem. Soc. Rev.*, 2012, vol. 41, pp. 666–686. https://doi.org/10.1039/c1cs15078b
29. Yu, B., Wang, X., and Xing, W.Y., *Ind. Eng. Chem. Res.*,

2012, vol. 51, no. 45, pp. 14629–14636. https://doi.org/10.1021/ie3013852

30. Li, Y.L., Kuan, C.F., and Chen, C.H., *Mater. Chem. Phys.*, 2012, vol. 134, pp. 677–695. https://doi.org/10.1016/j.matchemphys.2012.03.050
31. Wang, X., Xing, W.Y., and Zhang, P., *Compos. Sci. Technol.*, 2012, vol. 72, pp. 737–743. https://doi.org/10.1016/j.compscitech.2012.01.027
32. Liao, S.H., Liu, P.L., and Hsiao, M.C., *Ind. Eng. Chem. Res.*, 2012, vol. 51, no. 12, pp. 4573–4581. https://doi.org/10.1021/ie2026647
33. Bao, C.L., Guo, Y.Q., and Yuan, B.H., *J. Mater. Chem.*, 2012, vol. 22, no. 43, pp. 23057–23063. https://doi.org/10.1039/c2jm35001g
34. Georgakilas, V., Otyepka, M., and Bourlinos, A.B., *Chem. Rev.*, 2012, vol. 112, no. 11, pp. 6156–6214. https://doi.org/10.1021/cr3000412
35. Hu, W.Z., Zhan, J., and Wang, X., *Ind. Eng. Chem. Res.*, 2014, vol. 53, pp. 3073–3083. https://doi.org/10.1021/ie5010306
36. Qian, X.D., Pan, H.F., and Xing, X.Y., *Ind. Eng. Chem. Res.*, 2012, vol. 51, pp. 85–94. https://doi.org/10.1021/ie2017493
37. Marcano, D.C., Kosynkin, D.V., and Berlin, J.M., *ACS Nano*, 2010, vol. 4, no. 8, pp. 4806–4814. https://doi.org/10.1021/nn1006368
38. Xue, Y.H., Liu, Y., and Lu, F., *J. Phys. Chem. Lett.*, 2012, vol. 3, no. 12, pp. 1607–1612. https://doi.org/10.1021/jz3005877
39. Huang, G.B., Chen, S.Q., and Tang, S.W., *Mater. Chem. Phys.*, 2012, vol. 135, nos. 2–3, pp. 938–947. https://doi.org/10.1016/j.matchemphys.2012.05.082
40. Wang, X., Song, L., and Yang, H.Y., *J. Mater. Chem.*, 2012, vol. 22, pp. 22037–22043. https://doi.org/10.1039/c2jm35479a
41. Wang, X., Xing, W.Y., and Feng, X.M., *Polym. Chem.*, 2014, vol. 5, pp. 1145–1154. https://doi.org/10.1039/c3py00963g